



HAL
open science

Verifying Weakly-Hard Real-Time Properties of Traffic Streams in Switched Networks

Leonie Ahrendts, Sophie Quinton, Thomas Boroske, Rolf Ernst

► **To cite this version:**

Leonie Ahrendts, Sophie Quinton, Thomas Boroske, Rolf Ernst. Verifying Weakly-Hard Real-Time Properties of Traffic Streams in Switched Networks. ECRTS 2018 - 30th Euromicro Conference on Real-Time Systems, Jul 2018, Barcelona, Spain. pp.1-22, 10.4230/LIPIcs.ECRTS.2018.15. hal-01903759

HAL Id: hal-01903759

<https://inria.hal.science/hal-01903759v1>

Submitted on 24 Oct 2018

HAL is a multi-disciplinary open access archive for the deposit and dissemination of scientific research documents, whether they are published or not. The documents may come from teaching and research institutions in France or abroad, or from public or private research centers.

L'archive ouverte pluridisciplinaire **HAL**, est destinée au dépôt et à la diffusion de documents scientifiques de niveau recherche, publiés ou non, émanant des établissements d'enseignement et de recherche français ou étrangers, des laboratoires publics ou privés.

Verifying Weakly-Hard Real-Time Properties of Traffic Streams in Switched Networks

Leonie Ahrendts

Institute for Network and Computer Engineering, TU Braunschweig, Braunschweig, Germany
ahrendts@ida.ing.tu-bs.de

Sophie Quinton

Inria Grenoble Rhône-Alpes, Montbonnot, France
sophie.quinton@inria.fr

Thomas Boroske

Institute for Network and Computer Engineering, TU Braunschweig, Braunschweig, Germany
thomasb@ida.ing.tu-bs.de

Rolf Ernst

Institute for Network and Computer Engineering, TU Braunschweig, Braunschweig, Germany
ernst@ida.ing.tu-bs.de

Abstract

In this paper, we introduce the first verification method which is able to provide weakly-hard real-time guarantees for tasks and task chains in systems with multiple resources under partitioned scheduling with fixed priorities. Existing weakly-hard real-time verification techniques are restricted today to systems with a single resource. A weakly-hard real-time guarantee specifies an upper bound on the maximum number m of deadline misses of a task in a sequence of k consecutive executions. Such a guarantee is useful if a task can experience a bounded number of deadline misses without impacting the system mission. We present our verification method in the context of switched networks with traffic streams between nodes, and demonstrate its practical applicability in an automotive case study.

2012 ACM Subject Classification Computer systems organization → Embedded systems, Computer systems organization → Real-time systems, Software and its engineering → Formal software verification, Networks → Network performance analysis

Keywords and phrases embedded and cyber-physical systems, weakly-hard real-time systems and networks, timing analysis

Digital Object Identifier 10.4230/LIPIcs.ECRTS.2018.15

Funding This work has received funding from the German Research Foundation under the contract number 168/30-2.

1 Introduction

Modern embedded systems often have a distributed hardware platform, where the individual processing resources are linked by data buses or switched networks. A software application, which is mapped to such a platform, consists of a set of communicating tasks and has often to provide results within a limited response time. Timely communication between sender and receiver tasks is therefore a critical aspect in design and verification. In this paper, we concentrate on the timing behavior of traffic streams in switched networks like Switched Ethernet. By traffic stream we understand an infinite sequence of data transmissions between a sender and a receiver node of the network.



© Leonie Ahrendts, Sophie Quinton, Thomas Boroske and Rolf Ernst;
licensed under Creative Commons License CC-BY

30th Euromicro Conference on Real-Time Systems (ECRTS 2018).

Editor: Sebastian Altmeyer; Article No. 15; pp. 15:1–15:22

Leibniz International Proceedings in Informatics



LIPIC Schloss Dagstuhl – Leibniz-Zentrum für Informatik, Dagstuhl Publishing, Germany

42 If the classical hard real-time paradigm is applied to a traffic stream, then the duration of
 43 a data transmission over the network must not violate a given end-to-end deadline. However,
 44 with increasing functionality and growing bandwidth demand of data transmission in modern
 45 embedded systems in the automotive or industrial domain, it becomes more and more difficult
 46 to fulfill the end-to-end deadlines of all traffic streams in unfavorable scheduling scenarios. A
 47 promising option is the shift to the weakly-hard real-time paradigm [1] which relaxes these
 48 timing requirements. Here a traffic stream is feasible from a timing perspective, if it does
 49 not exceed a certain budget of end-to-end deadline misses. For instance, a traffic stream may
 50 not miss more than m end-to-end deadlines in any k consecutive transmissions. The traffic
 51 stream is said to be (m, k) -constrained.

52 The practical justification of weakly-hard real-time paradigm in the context of communic-
 53 ation builds on the observed robustness of many real-time software systems. In the field of
 54 image processing, a late transmission may result in a skipped frame. Given that the number
 55 and distribution of frame skips is appropriately bounded, it will not be noticeable to the
 56 human eye. In the field of control, an end-to-end deadline miss may cause the calculation of
 57 the control law to fail at time instant k so that no new control input is sent to the actuator
 58 at this instant. Several works could show that under given (m, k) -constraints the required
 59 control performance could be maintained [15] [9] [8]. Blind et al. [2] could show stability
 60 in the classical sense of Lyapunov for a networked control system, where the network is
 61 unreliable in the (m, k) -sense.

62 So far, verification techniques have been developed which allow to derive (m, k) -guarantees
 63 for tasks which are executed on a system with a *single* service-providing resource. A switched
 64 network, however, comprises *several* service-providing resources as detailed in Section 2.
 65 In this paper, we therefore provide a compositional verification method which is able to
 66 provide (m, k) -guarantees for multi-resource problems. The main challenge in extending an
 67 existing (m, k) -verification method to the multi-resource setting is to deal with inter-resource
 68 dependencies. Our approach builds on both

- 69 1. *Compositional Performance Analysis (CPA)*. CPA [11] is a compositional framework to
 70 verify classical hard real-time properties, e.g., worst case response times. It deals with
 71 inter-resource dependencies by the formulation of a fixed-point problem.
- 72 2. *Typical Worst Case Analysis (TWCA)* TWCA [21] is one of the existing (m, k) -verification
 73 techniques for single resource systems.

74 We adapt and extend CPA and TWCA, calling the resulting procedure *TypicalCPA*. The
 75 paper is structured as follows. We begin by defining our system model, and then introduce
 76 the CPA approach. We continue by explaining the basic principle of TWCA, and reason how
 77 CPA and TWCA can be coupled. Finally, we perform and discuss experiments. An overview
 78 of related work is given before the conclusion.

79 **2 Network Model**

80 The system model represents a real-time network setting with unicast, multicast and broadcast
 81 streams and is depicted in Figure 1. The scope of the model includes, for instance, Switched
 82 Ethernet but is not limited to it. The main components of the network model are switches
 83 and nodes. A pair of nodes may communicate by sending frames over the network which
 84 are forwarded by the switches using appropriate output ports. The service of output ports
 85 for frame transmission is scarce and has to be arbitrated according to a static priority

86 non-preemptive (SPNP) scheduling policy. The output ports therefore represent the service-
87 providing resources R_k in the system [6].

88 An infinite sequence of frames between a source node and 1 [a subset of resp. all]
89 destination node(s) is called a unicast [multicast resp. broadcast] stream. A unicast [multicast
90 resp. broadcast] stream s_i is modeled as a linear [forked] chain of N tasks, where each task
91 represents a hop in the route and is mapped to the output port of the respective switch. We
92 call the set of N tasks contained in the stream s_i $\mathcal{T}_{s_i} = \{\tau_{i,1}, \tau_{i,2}, \dots, \tau_{i,N}\}$ and define the
93 respective precedence constraints, e.g. for a unicast stream as $\tau_{i,1} \prec \tau_{i,2} \prec \dots \prec \tau_{i,N}$. The
94 first task in the stream s_i , is activated by an external event source. All successor tasks are
95 activated by the termination events of their respective predecessor task in the chain. Each
96 task $\tau_{i,j}$ in stream s_i has a non-unique priority p_i . The best case execution time (BCET)
97 resp. worst case execution time (WCET) of task $\tau_{i,j}$, denoted as $C_{i,j}^-$ resp. $C_{i,j}^+$, represents
98 the minimum resp. maximum frame delay in the switch plus the constant wire transmission
99 time, and is independent of other traffic in the network. Dynamic delays resulting from
100 contention at the switch output ports are considered in the response time computation of
101 tasks. The maximum response time of a task $\tau_{i,j}$ is constrained by the relative deadline
102 $d_{i,j}$, while the maximum network traversal time w.r.t. a stream s_i should not exceed the
103 end-to-end deadline $D_i = \sum_j d_{i,j}$.

104 We describe the occurrence of activation events over time w.r.t. a task $\tau_{i,j}$ by the concept
105 of event flows as well as by minimum and maximum event models.

106 ► **Definition 1** (Event flow). An event flow $e_{i,j}(t)$ is a function which returns the number of
107 events which activate task $\tau_{i,j}$ within the time interval $[0, t)$ in a given execution run.

108 ► **Definition 2** (Event model). The minimum and maximum event models $\eta_{i,j}^-(\Delta t)$ and
109 $\eta_{i,j}^+(\Delta t)$ indicate a lower and upper bound, respectively, on the number of activation events
110 for task $\tau_{i,j}$ in any time interval $[t, t + \Delta t)$. Any event flow $e_{i,j}(t)$ of task $\tau_{i,j}$ is therefore
111 constrained by

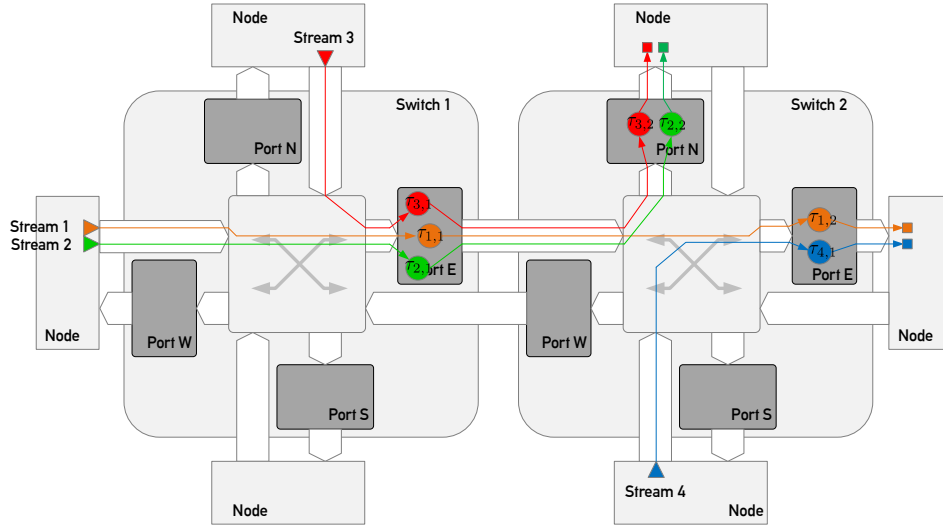
$$112 \quad \forall t_1, t_2 : t_1 \leq t_2 : \eta_{i,j}^-(t_2 - t_1) \leq e_{i,j}(t_2) - e_{i,j}(t_1) \leq \eta_{i,j}^+(t_2 - t_1).$$

114 If convenient, we also use the pseudo-inverses of event models, i.e., the event distance
115 functions. The event distance function $\delta_{i,j}^-(n)$ [$\delta_{i,j}^+(n)$] is the pseudo-inverse of event model
116 $\eta_{i,j}^+(\Delta t)$ [$\eta_{i,j}^-(\Delta t)$].

117 ► **Definition 3** (Event distance functions). The minimum and maximum distance functions
118 $\delta_{i,j}^-(n)$ and $\delta_{i,j}^+(n)$ indicate a lower and upper bound, respectively, on the temporal distance
119 between the first and the last event of a sequence of n activation events for task $\tau_{i,j}$. For the
120 special case $n \in \{0, 1\}$, the definition $\delta_{i,j}^-(n) = \delta_{i,j}^+(n) = 0$ applies.

121 **3 Compositional Performance Analysis**

122 CPA [11] is a verification framework which derives lower and upper bounds on the timing
123 properties of distributed real-time software systems with partitioned scheduling. Computed
124 timing properties include in particular the best case response times (BCRTs) and worst case
125 response times (WCRTs) of tasks. CPA is implemented in Python as pyCPA [4], the basic
126 libraries of pyCPA are available on-line [5]. The CPA method breaks the verification problem
127 down into a set of local, i.e. resource-related, analysis problems. A subsequent analysis step
128 then relates the local verification problems such that inter-resource dependencies are taken
129 into account and a global fixed point problem is formulated.

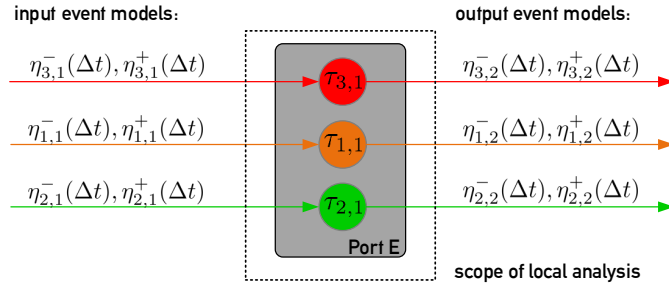


■ **Figure 1** Network model. The figure illustrates a network with six nodes and two switches. The output ports of a switch are named after the points of the compass. Four exemplary unicast streams are represented.

130 ► **Definition 4** (Attributes local & global). The attribute «local» refers to parameters,
 131 properties etc. of a specific resource R_k and the associated (mapped) task set \mathcal{T}_{R_k} .
 132 The attribute «global» refers, on the contrary, to parameters, properties etc. of the processing
 133 platform $\mathcal{P} = \bigcup_k R_k$ and the entire task set $\mathcal{T} = \bigcup_k \mathcal{T}_{R_k}$.

134 3.1 Local Analysis

135 The local analysis focuses on the isolated resource R_k and derives the timing properties of
 136 the associated task set \mathcal{T}_{R_k} . The analysis objective is in particular to compute (a) the BCRT
 and WCRT for each task $\tau_{i,j} \in \mathcal{T}_{R_k}$, and (b) the output event model of each task $\tau_{i,j} \in \mathcal{T}_{R_k}$.



■ **Figure 2** Scope and interface of the local CPA. The figure shows as an example the output port E of switch 1 with mapped tasks.

137

138 3.1.1 Computation of Response Times

139 In the following, we very briefly sketch the response time analysis for a task $\tau_{i,j}$ which is
 140 mapped to an SPNP-scheduled resource R_k . For a detailed presentation, please refer to [7].
 141 To find the WCRT of task $\tau_{i,j}$, a scheduling scenario has to be known which induces the

142 longest response time of task $\tau_{i,j}$. This worst case scenario is often called the *maximum*
 143 *level- $\tau_{i,j}$ busy period*. It is known to start if $\tau_{i,j} \cup hsp(\tau_{i,j})^1$ are activated synchronously and a
 144 task in $lp(\tau_{i,j})$, which has just been activated before, causes the maximum blocking delay [3].
 145 It closes as soon as the resource becomes idle w.r.t. $\tau_{i,j}$ and $hsp(\tau_{i,j})$ -tasks. The processing
 146 behavior of task $\tau_{i,j}$ within the maximum level- $\tau_{i,j}$ busy period can be described by the so
 147 called *multiple event busy times* $B_{i,j}^+(q)$.

148 ► **Definition 5.** The maximum q -event busy time $B_{i,j}^+(q)$ indicates the processing time of q
 149 consecutive activation events of task $\tau_{i,j}$ within the maximum level- $\tau_{i,j}$ busy period. $B_{i,j}^+(q)$
 150 always starts with the beginning of the maximum level- $\tau_{i,j}$ busy period [17].

151 The busy times $B_{i,j}^+(q)$ depend on the input event models and WCETs of the tasks \mathcal{T}_{R_k} . It
 152 has been shown that the WCRT $R_{i,j}^+$ of task $\tau_{i,j}$ is among its response times in the maximum
 153 level- $\tau_{i,j}$ busy period, such that we can write

$$154 \quad R_{i,j}^+ = \max_{1 \leq q \leq K_{i,j}} \{B_{i,j}^+(q) - \delta_{i,j}^-(q)\} \quad (1)$$

156 where $K_{i,j}$ is the maximum number of jobs of task $\tau_{i,j}$ contained in the maximum level- $\tau_{i,j}$
 157 busy period. The BCRT of task $\tau_{i,j}$ can be approximated by its BCET $R_{i,j}^- = C_{i,j}^-$.

158 3.1.2 Computation of Output Event Distance Functions and Output 159 Event Models

160 The local analysis problems are linked because precedence relations extend over tasks on
 161 different resources as illustrated in Figure 1. According to the synchronous task chain
 162 semantics, a termination event of a task $\tau_{i,j}$ is interpreted as an activation event by the
 163 successor task $\tau_{i,j+1}$. This interaction between tasks $\tau_{i,j}$ and $\tau_{i,j+1}$ can be quantified by
 164 the distance functions $\delta_{i,j+1}^+(n)$ resp. $\delta_{i,j+1}^-(n)$ indicating the maximum resp. minimum
 165 number of distance between any n consecutive termination events of task $\tau_{i,j}$ or, equivalently,
 166 activation events of task $\tau_{i,j+1}$. Firstly, let us present safe, easy-to-interpret bounds for the
 167 distance functions with $n \geq 2$ using the *jitter method* [16]

$$168 \quad \delta_{i,j+1}^-(n) \geq \max \{ (n-1) \cdot C_{i,j}^-, \delta_{i,j}^-(n) - J_{i,j}^+ \} \quad (2)$$

$$169 \quad \delta_{i,j+1}^+(n) \leq \delta_{i,j}^+(n) + J_{i,j}^+ \quad (3)$$

171 Eq. 2 expresses that, in the worst case, n termination events at the output of task $\tau_{i,j}$ are
 172 closer by the maximum response time jitter $J_{i,j}^+ = R_{i,j}^+ - R_{i,j}^-$ than n activation events at
 173 the input of the same task. Also, the density of activation events increases with every stage
 174 of the task chain due to the accumulation of response jitter. Eq. 3 describes that, in the
 175 best case, the distance of n termination events grows with every stage of a task chain by the
 176 jitter $J_{i,j}^+$. Secondly, we introduce more accurate but less intuitive bounds which have been
 177 derived in [18] (*busy window method*)

$$178 \quad \delta_{i,j+1}^-(n) \geq \max \{ B_{i,j}^-(n-1), \min_{1 \leq q \leq q_{i,j}^+} \{ \delta_{i,j}^-(n+q-1) - B_{i,j}^+(q) \} + B_{i,j}^-(1) \} \quad (4)$$

$$179 \quad \delta_{i,j+1}^+(n) \leq \max_{1 \leq q \leq q_i^+} \{ \delta_{i,j}^+(n-q+1) + B_{i,j}^+(q) \} - B_{i,j}^-(1). \quad (5)$$

180

¹ We use $hsp(\tau_{i,j})$ to denote the set of tasks which have *higher or same priority* than task $\tau_{i,j} \in \mathcal{T}_{R_k}$ and are mapped to the same resource R_k . Likewise we write $lp(\tau_{i,j})$ to denote the set of tasks which have *lower priority* than task $\tau_{i,j} \in \mathcal{T}_{R_k}$ and are mapped to the same resource R_k .

181 According to the rules of network calculus [12], the event distance function $\delta_{i,j+1}^-(n)$ resp.
 182 $\delta_{i,j+1}^+(n)$ can even be more improved in accuracy if replaced by its superadditive closure
 183 $\bar{\delta}_{i,j+1}^-(n)$ resp. subadditive closure $\bar{\delta}_{i,j+1}^+(n)$. In the following, we continue to write $\delta_{i,j+1}^-(n)$
 184 resp. $\delta_{i,j+1}^+(n)$ (without bar) stating explicitly when we make use of the superadditivity
 185 property ($\delta_{i,j+1}^-(m+n) \geq \delta_{i,j+1}^-(m) + \delta_{i,j+1}^-(n)$) or subadditivity property ($\delta_{i,j+1}^+(m+n) \leq$
 186 $\delta_{i,j+1}^+(m) + \delta_{i,j+1}^+(n)$). Note again that the output event models $\eta_{i,j+1}^+(\Delta t)$, $\eta_{i,j+1}^-(\Delta t)$ can
 187 be obtained from the output event distance functions by pseudo-inversion.

188 It is desirable for efficiency reasons to have a finite representation of event distance
 189 functions, meaning that it is possible to construct the event distance functions for every n
 190 on the basis of a limited number of l known points. This can be achieved by approxim-
 191 ating $\delta_{i,j+1}^-(n)$, $\delta_{i,j+1}^+(n)$ by bounds with a repetitive behavior. The approximation is very
 192 acceptable with regard to accuracy, if the repetition period is chosen large enough. In the
 193 particular context of this paper, repetitive bounds restrict the value range that needs to be
 194 processed by the algorithm given in Theorem 23. We concentrate in the following on $\delta^-(n)$
 195 and its pseudo-inverse $\eta^+(\Delta)$, but analogous rules can be applied to $\delta^+(n)$ and $\eta^-(\Delta)$.

196 ► **Lemma 6** (Repetitive extension of an event distance function). *Given the superadditive event*
 197 *distance function $\delta^-(n)$ for $1 \leq n \leq l$, an l -repetitive extension $\hat{\delta}^-(n)$ is defined by*

$$198 \quad \hat{\delta}^-(n) = \begin{cases} 0 & \text{for } 0 \leq n \leq 1 \\ \lfloor \frac{n-2}{l} \rfloor \cdot \delta^-(l) + \delta^-(n - \lfloor \frac{n-2}{l} \rfloor \cdot l) & \text{for } n \geq 2. \end{cases}$$

200 *The l -repetitive extension $\hat{\delta}^-(n)$ is a lower bound for $\delta^-(n)$, s.t. $\forall n : \hat{\delta}^-(n) \leq \delta^-(n)$.*

201 **Proof.** We have $\hat{\delta}^-(n) = \delta^-(n) = 0$ for $n \in \{0, 1\}$, and $\hat{\delta}^-(n) = \delta^-(n)$ for $2 \leq n \leq l + 2$.
 202 For $n > l + 2$, we make use of the superadditivity property $\delta^-(n_1) + \delta^-(n_2) \leq \delta^-(n_1 + n_2)$
 203 and set $x = \lfloor \frac{n-2}{l} \rfloor$: $\hat{\delta}^-(n) = x \cdot \delta^-(l) + \delta^-(n - x \cdot l) \leq \delta^-(x \cdot l) + \delta^-(n - x \cdot l) \leq \delta^-(n)$. ◀

204 ► **Lemma 7** (Repetitive extension of an event model). *Given the subadditive event model*
 205 *function $\eta^+(\Delta t)$, a T -repetitive extension $\hat{\eta}_l^+(\Delta t)$ is defined by*

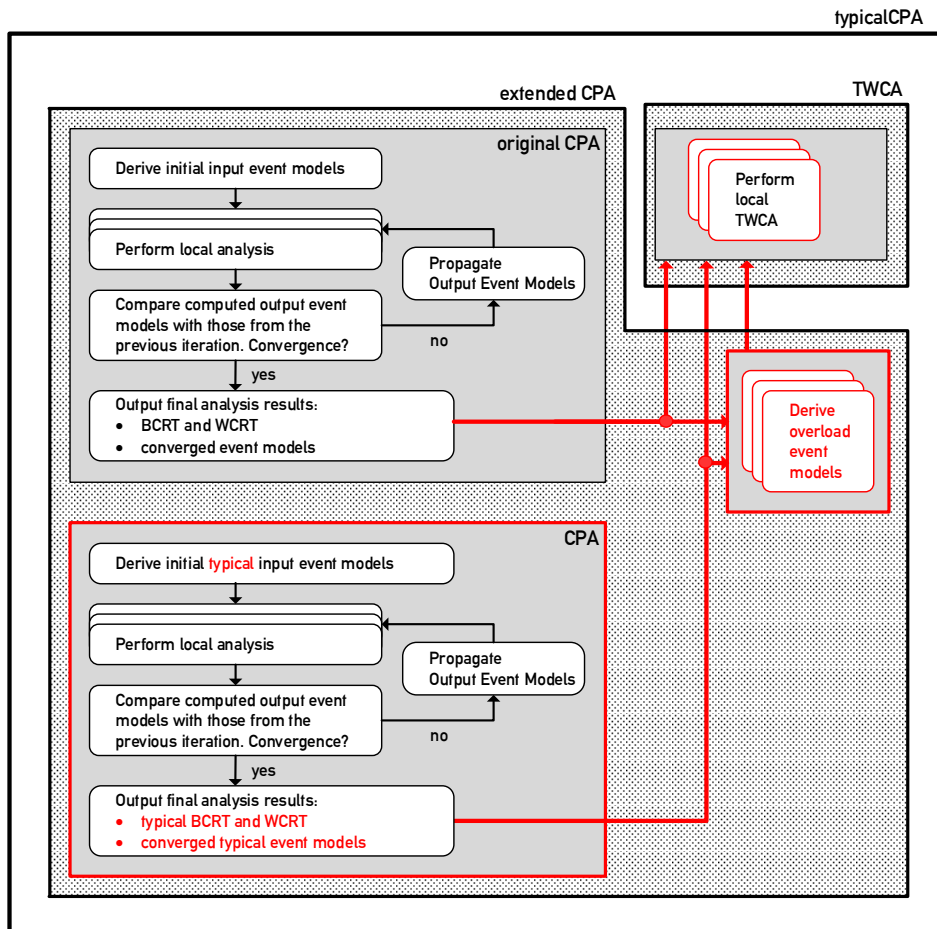
$$206 \quad \hat{\eta}_l^+(\Delta t) = \left\lfloor \frac{\Delta t}{T} \right\rfloor \cdot \eta^+(T) + \eta^+(\Delta t - \left\lfloor \frac{\Delta t}{T} \right\rfloor \cdot T).$$

208 *If $\hat{\delta}^-(n)$ is l -repetitive, then its pseudo-inverse $\hat{\eta}_l^+(\Delta t)$ must be $T = \hat{\delta}^-(l)$ -repetitive.*

209 **Proof.** This results from the symmetry of function inversion. ◀

210 3.2 Global Analysis

211 The global analysis now couples the local analysis problems according to the following iterative
 212 procedure, which is also depicted in Figure 3 (box entitled “original CPA”). Firstly, each
 213 header task of a stream $\tau_{i,1}$ has a known activation behavior bounded by $\eta_{i,1}^-(\Delta t)$, $\eta_{i,1}^+(\Delta t)$
 214 and imposed by external event sources. Since initially no event models are available for
 215 successor tasks in the stream, i.e. for $\tau_{i,j}$ with $j > 1$, they are initialized with the event model
 216 assigned to the header task $\tau_{i,1}$. The local analysis is then performed for each resource, such
 217 that response time bounds and output event models are obtained. The computed output
 218 event models are then *propagated* to the direct successor tasks, where they are interpreted as
 219 input event models. The local analysis is then repeated with the updated event models. If
 220 all propagated event models are identical to the event models used in the previous analysis
 221 run, a global fixed point is reached and the analysis terminates.



■ **Figure 3** TypicalCPA. The extended CPA also derives typical and overload event models as detailed in Section 5, which are then processed by a TWCA for each component. New or adapted elements of CPA and TWCA are marked in red.

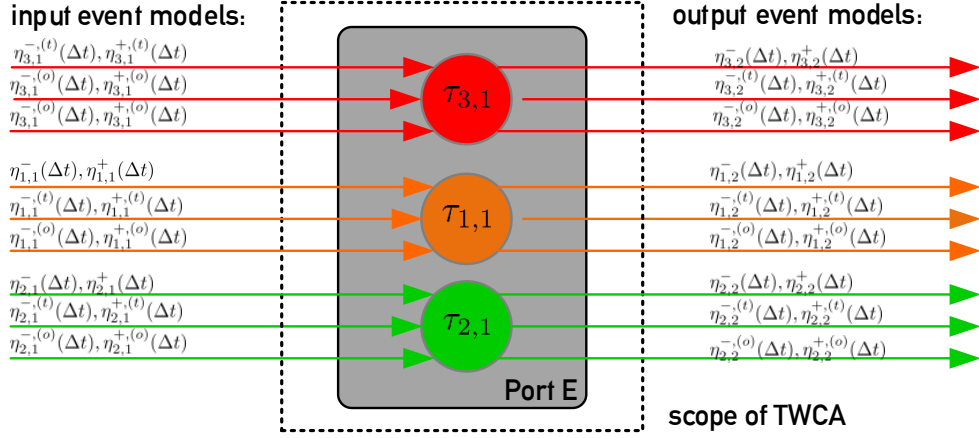
4 Typical Worst Case Analysis

Typical Worst Case Analysis (TWCA) models and analyzes systems with a single service-providing resource R_k under transient overload conditions. It provides weakly-hard real-time guarantees for tasks \mathcal{T}_{R_k} . In this section, we firstly present which extensions to the CPA system model presented in Section 2 are necessary to apply TWCA. Then the TWCA procedure is introduced together with a needed generalization of a schedulability criterion.

4.1 Extended System Model

The system model of CPA presented in Section 2 is a subset of the TWCA system model. The important extension of the CPA model by TWCA is that each task $\tau_{i,j}$ may be activated by events of two distinct classes, namely by *typical and overload events*. The idea is that in the exclusive presence of typical events, the task set \mathcal{T}_{R_k} is schedulable. In contrast, the supplementary overload events are a potential cause for transient overload.

► **Definition 8** (Local typical worst case). If every task $\tau_{i,j} \in \mathcal{T}_{R_k}$ is only activated by typical



■ **Figure 4** Scope and interface of TWCA.

235 events, then the task set \mathcal{T}_{R_k} is schedulable even in the most unfavorable scheduling scenario
 236 (*local typical worst case*).

237 ► **Definition 9** (Local worst case). If every task $\tau_{i,j} \in \mathcal{T}_{R_k}$ is activated by both typical and
 238 overload events, then in the most unfavorable scheduling scenario (*local worst case*) the task
 239 set \mathcal{T}_{R_k} is possibly unschedulable.

240 The occurrence of typical or overload activation events over time w.r.t. a task $\tau_{i,j}$ is also
 241 modeled by the concept of event flows, while the minimum and maximum frequency of typical
 242 and overload event arrival is described by event models. The corresponding definitions are
 243 given below, while Figure 4 shows the extended system model with the additional event
 244 models.

245 ► **Definition 10** (Typical and overload event flows). A typical event flow $e_{i,j}^{(t)}(t)$, resp. overload
 246 event flow $e_{i,j}^{(o)}(t)$, is a function which returns the number of typical, resp. overload,
 247 events which activate task $\tau_{i,j}$ within the time interval $[0, t)$ in a given execution run.

248 ► **Definition 11** (Typical and overload event models). The event models $\eta_{i,j}^{-(t)}(\Delta t), \eta_{i,j}^{+(t)}(\Delta t)$,
 249 resp. $\eta_{i,j}^{-(o)}(\Delta t), \eta_{i,j}^{+(o)}(\Delta t)$, indicate a lower and an upper bound on the number of typical,
 250 resp. overload, events which activate task $\tau_{i,j}$ within Δt .

251 ► **Definition 12** (Decomposition). Any observed event flow of task $\tau_{i,j}$ which satisfies the
 252 lower and upper bounds $\eta_{i,j}^-(\Delta t), \eta_{i,j}^+(\Delta t)$ can be partitioned in

- 253 (1) an event flow of typical events satisfying $\eta_{i,j}^{-(t)}(\Delta t), \eta_{i,j}^{+(t)}(\Delta t)$ and
- 254 (2) an event flow of overload events satisfying $\eta_{i,j}^{-(o)}(\Delta t), \eta_{i,j}^{+(o)}(\Delta t)$.

255 This implies that the maximum event model $\eta_{i,j}^+(\Delta t)$ is *decomposable*, s.t. $\eta_{i,j}^+(\Delta t) \leq$
 256 $\eta_{i,j}^{+(t)}(\Delta t) + \eta_{i,j}^{+(o)}(\Delta t)$. If $\eta_{i,j}^+(\Delta t) = \eta_{i,j}^{+(t)}(\Delta t) + \eta_{i,j}^{+(o)}(\Delta t)$ holds, then the maximum event
 257 model is said to be *exactly decomposable*. Please refer for illustration to Figure 5c.

258 The intuition related to the system model is that a computing platform may be designed
 259 to provide sufficient processing service for a typical workload. For instance, if all tasks have
 260 a periodic (= typical) activation pattern, then the task set is schedulable. If, however, some
 261 tasks experience additional sporadic (= overload) activations, then the task set may become
 262 unschedulable in unfavorable scheduling scenarios.

4.2 Basic Procedure

The objective of TWCA is to determine weakly-hard real-time guarantees for all tasks in the task set. More precisely, a deadline miss model (DMM) is obtained for every task $\tau_{i,j} \in \mathcal{T}_{R_k}$.

► **Definition 13** (Deadline miss model). A deadline miss model for a task $\tau_{i,j}$ is a function $dmm_{i,j} : \mathbb{N} \rightarrow \mathbb{N}$ with the property that out of any k consecutive jobs of task $\tau_{i,j}$, at most $dmm_{i,j}(k)$ might miss their deadline $d_{i,j}$.

To compute $dmm_{i,j}(k)$ under SPNP scheduling, TWCA quantifies the impact of overload activations. We summarize the procedure in the following steps.

1. Firstly TWCA derives the maximum impact which a single overload activation of a task $\tau_{m,n} \in \text{hsp}(\tau_{i,j})$ can have on the task $\tau_{i,j}$. The impact is counted by the maximum number jobs of task $\tau_{i,j}$ which can miss their deadline due to this overload activation, and is denoted as $N_{i,j}$.
2. It is computed how many overload activations of task $\tau_{m,n}$ can at most influence the k -sequence of task $\tau_{i,j}$. This number is given by $\eta_{m,n}^{+, (o)}(\Delta T_k^{i,j})$, where $\Delta T_k^{i,j}$ describes the maximum time interval during which a k -sequence of task $\tau_{i,j}$ is sensitive to overload events.
3. The overall impact of task $\tau_{m,n}$ is then derived as the product $N_{i,j} \cdot \eta_{m,n}^{+, (o)}(\Delta T_k^{i,j})$.
4. Finally, the impact of all $\tau_{m,n}$ tasks which may interfere with task $\tau_{i,j}$ is summed. Interfering tasks have higher or same priority (hsp) than task $\tau_{i,j}$.

Thus we have

$$dmm_{i,j}(k) = \sum_{\tau_{m,n} \in \text{hsp}(\tau_{i,j})} N_{i,j} \cdot \eta_{m,n}^{+, (o)}(\Delta T_k^{i,j}) \quad (6)$$

where

$$N_{i,j} = \# \{q \in \mathbb{N}^+ \mid 1 \leq q \leq K_{i,j} \wedge d_{i,j} < R_{i,j}^+(q)\} \quad (7)$$

$$\Delta T_k^{i,j} \leq B_{i,j}^+(K_{i,j}) + \delta_{i,j}^+(k) + (R_{i,j}^+ - C_{i,j}^+) \quad (8)$$

Please refer for a detailed explanation to [10].

4.3 Improved Procedure

The presented basic TWCA assumes that *every* isolated overload activation of a task $\tau_{m,n}$ which interferes with task $\tau_{i,j}$ causes at most $N_{i,j}$ deadline misses. The approach presented in [21] improves over the basic TWCA by considering that often actually the *combined* effect of overload from several interferer tasks is required to cause a deadline miss of task $\tau_{i,j}$. We introduce therefore the following definitions.

► **Definition 14** (Combination). A local combination $C \subseteq \mathcal{T}_{R_k}$ is a set of tasks which may experience both typical as well as overload activation events, whereas the tasks of the complementary set, $\mathcal{T}_{R_k} \setminus C$, experience only typical activation events.

► **Definition 15** (Unschedulable combinations). $R_{i,j}^{+, C}$ denotes the longest response time of task $\tau_{i,j} \in \mathcal{T}_R$, assuming that only tasks in C experience overload activations. A combination C is said to be schedulable w.r.t. to task $\tau_{i,j}$, if $R_{i,j}^{+, C} \leq d_{i,j}$, otherwise it is unschedulable. The set of unschedulable combinations w.r.t. to task $\tau_{i,j}$ is called $\mathcal{U}_{i,j}$.

302 Note that special local combinations are $C = \emptyset$ and $C = \mathcal{T}_{R_k}$. In this context, $R_{i,j}^{+, \mathcal{T}_{R_k}}$ is the
 303 usual worst case response time and $R_{i,j}^{+, \emptyset}$ is called typical worst case response time.

304 The improved TWCA [21] is now based on the fact that the sensitivity interval $\Delta T_k^{i,j}$ of
 305 the k -sequence of task $\tau_{i,j}$ can be divided into a sequence of busy periods [13]. The timing
 306 behavior of busy periods is mutually independent, because of the idle times which separate
 307 them. Within in any such busy period, an unschedulable combination is necessary to cause
 308 at most $N_{i,j}$ deadline misses of task $\tau_{i,j}$ within this interval. A single task $\tau_{m,n}$ can be part
 309 of unschedulable combinations at most $\Omega_{m,n} = \eta_{m,n}^{+, (o)}(\Delta T_k^{i,j})$ times, which corresponds to
 310 the maximum number of overload activations in $\Delta T_k^{i,j}$.

311 Let $x_C \in \mathbb{N}$ count the number of busy periods in $\Delta T_k^{i,j}$, which suffer from an unschedulable
 312 combination $C \in \mathcal{U}_{i,j}$. Then the DMM can be obtained by solving the following optimization
 313 problem

$$314 \quad dmm_{i,j}(k) = \max N_{i,j} \sum_{C: C \in \mathcal{U}_{i,j}} x_C \quad (9)$$

$$315 \quad \text{s.t.} \quad \sum_{C, (m,n)} x_C \leq \Omega_{m,n} \quad (10)$$

$$316 \quad \text{with } C, (m,n) : (\tau_{m,n} \in hsp(\tau_{i,j}) \cup \tau_{i,j}) \wedge (\tau_{m,n} \in C) \wedge (C \in \mathcal{U}_{i,j})$$

318 To determine whether a combination C is schedulable or not, a fast schedulability criterion
 319 is required. We rely on the criterion presented in [21], but generalize it for (1) non-unique
 320 priorities, and (2) the general relation where the maximum event models are not exactly
 321 decomposable. The generalization is presented in Theorem 16; notation and explanations of
 322 the theorem contents are given in the corresponding proof and Figure 5.

323 ► **Theorem 16** (Generalized schedulability criterion). *Equation 11 formulates a schedulability*
 324 *criterion for task $\tau_{i,j}$ under a given combination C .*

$$325 \quad \forall l \in K_{i,j} : \sum_{\forall \tau_{m,n} : \tau_{m,n} \in hsp(\tau_{i,j}) \cup \tau_{i,j} \wedge \tau_{m,n} \notin C} w_{over}^{(m,n), l} \geq \Lambda_{i,j}^l - \Gamma_{i,j}^l. \quad (11)$$

327 The following abbreviations are used

$$328 \quad \Lambda_{i,j}^l = B_{i,j}^+(l) - \delta_{i,j}^-(l) - d_{i,j}$$

$$329 \quad \Gamma_{i,j}^l = \sum_{\tau_{m,n} \in hp(\tau_{i,j})} C_{m,n}^+ \cdot [\eta_{m,n}^+(B_{i,j}^+(l) - C_{i,j}^+) - \eta_{m,n}^+(\Delta t_{i,j}^l)]$$

$$330 \quad \Delta t_{i,j}^l = \delta_{i,j}^-(l) + d_{i,j} - C_{i,j}^+$$

$$331 \quad w_{over}^{(m,n), l} = \begin{cases} C_{m,n}^+ \cdot \left(\eta_{m,n}^+(\Delta t_{i,j}^l) - \eta_{m,n}^{+, (t)}(\Delta t_{i,j}^l) \right) & \text{for } \tau_{m,n} \in hp(\tau_{i,j}) \\ C_{m,n}^+ \cdot \left(\eta_{m,n}^+(\delta_{i,j}^-(l)) - \eta_{m,n}^{+, (t)}(\delta_{i,j}^-(l)) \right) & \text{for } \tau_{m,n} \in sp(\tau_{i,j}) \cup \tau_{i,j} \end{cases}$$

333 **Proof.** Let us verify the schedulability of task $\tau_{i,j}$ under a given combination C , i.e. we verify
 334 whether $R_{i,j}^{+, C} \leq d_{i,j}$ is true. We start from the unschedulable local worst case with $C' = \mathcal{T}_{R_k}$,
 335 which is represented by the maximum level- $\tau_{i,j}$ busy period which contains $K_{i,j}$ jobs of task
 336 $\tau_{i,j}$ (cf. Figure 5a). If the task $\tau_{i,j}$ is schedulable in the local worst case, then it schedulable
 337 for every combination and the problem is solved. If, however, task $\tau_{i,j}$ is unschedulable in
 338 the local worst case, then some of the $K_{i,j}$ jobs of task $\tau_{i,j}$ miss their deadline. The l th job
 339 of $\tau_{i,j}$ exceeds its deadline in the local worst case by (cf. also Figure 5)

$$340 \quad \Lambda_{i,j}^l = R_{i,j}^{+, C}(l) - d_{i,j} = B_{i,j}^+(l) - \delta_{i,j}^-(l) - d_{i,j}.$$

342 If its deadline is enforced by removing overload, an amount of workload $\Gamma_{i,j}^l$ will disappear
 343 automatically. Namely the workload from interfering activations which occur after the
 344 deadline but before the non-preemptive execution of the l th job. Jobs of tasks with the same
 345 priority (sp) as $\tau_{i,j}$ do not contribute to $\Gamma_{i,j}^l$, because they influence the response time of the
 346 l th job only if they have arrived earlier than or simultaneously with this job.

$$347 \quad \Gamma_{i,j}^l = \sum_{\tau_{m,n} \in hp(\tau_{i,j})} C_{m,n}^+ \cdot [\eta_{m,n}^+(B_{i,j}^+(l) - C_{i,j}^+) - \eta_{m,n}^+(\delta_{i,j}^-(l) + d_{i,j} - C_{i,j}^+)]$$

349 The RHS of inequality 11 describes the smallest amount of overload of interfering tasks that
 350 needs removed for sufficient schedulability of the l th job of $\tau_{i,j}$ in the maximum busy period.
 351 The LHS of Eq. 11 describes how much overload is removed compared to the local worst
 352 case, if we assume combination C (cf. Figure 5b for $C = \emptyset$). Under combination C , all tasks
 353 $\tau_{m,n} \notin C$ experience only typical activations and their overload is not present. In other
 354 words, the tasks $\tau_{m,n} \notin C$ follow their event model $\eta_{m,n}^{+, (t)}(\Delta t)$. In particular, an amount of
 355 overload per task $\tau_{m,n}$

$$356 \quad w_{over}^{(m,n),l} = \begin{cases} C_{i,j}^+ \cdot \left(\eta_{m,n}^+(\Delta t_{i,j}^l) - \eta_{m,n}^{+, (t)}(\Delta t_{i,j}^l) \right) & \text{for } \tau_{m,n} \in hp(\tau_{i,j}) \\ C_{i,j}^+ \cdot \left(\eta_{m,n}^+(\delta_i^-(l)) - \eta_{m,n}^{+, (t)}(\delta_i^-(l)) \right) & \text{for } \tau_{m,n} \in sp(\tau_{i,j}) \cup \tau_{i,j} \end{cases}$$

358 is removed which impacts the response time of the l th job of task $\tau_{i,j}$. Namely, the interfering
 359 overload of $hp(\tau_{i,j})$ -tasks until the timely nonpreemptive execution of job $\tau_{i,j}(l)$ is absent.
 360 Likewise, the overload of all $sp(\tau_{i,j})$ -jobs and overload jobs of $\tau_{i,j}$ are absent, which interfere
 361 if they arrive before or simultaneously with job $\tau_{i,j}(l)$.² ◀

362 5 Typical Compositional Performance Analysis

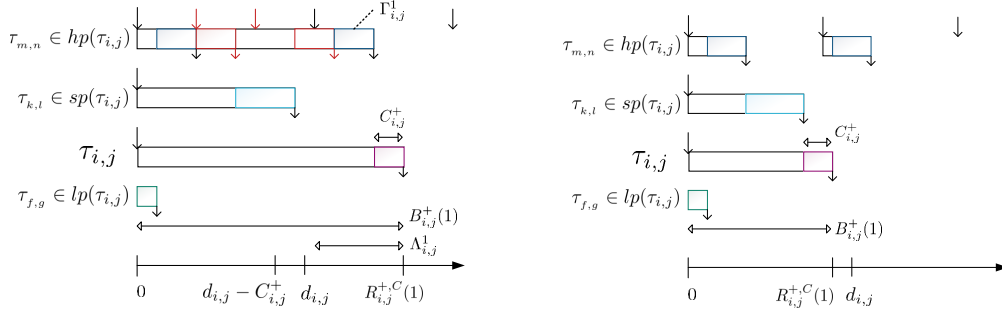
363 The new framework TypicalCPA, which we develop in this paper, combines CPA and TWCA
 364 such that weakly-hard real-time guarantees can be given for tasks in a multi-resource system.
 365 More concretely, the local analysis method TWCA will be performed for each component after
 366 an extended CPA has terminated. This is illustrated in Figure 3. To apply TWCA as a
 367 local analysis method, for each task minimum and maximum event models together with
 368 the corresponding minimum and maximum typical and overload event models have to be
 369 provided. The state-of-the-art CPA, however, computes as a result, besides BCRT and
 370 WCRT, so far only the converged minimum and maximum event models of each task (not
 371 their typical and overload variants) and thus has to be extended.

372 In the following we assume that the complete set of event models – $(\eta_{i,1}^-(\Delta t), \eta_{i,1}^+(\Delta t))$,
 373 $(\eta_{i,1}^{-(t)}(\Delta t), \eta_{i,1}^{+(t)}(\Delta t))$ and $(\eta_{i,1}^{-(o)}(\Delta t), \eta_{i,1}^{+(o)}(\Delta t))$ – is given for the header tasks $\tau_{i,1}$, since
 374 they are activated by external event sources. The problem to be addressed is how to derive
 375 these event models for all successor tasks in the context of CPA such that they can be used
 376 for the subsequent TWCA.

377 5.1 Basic Definitions

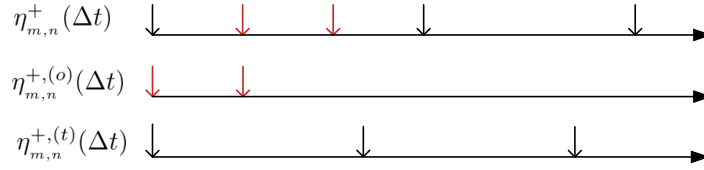
378 We begin by introducing the concept of a *global combination* describing the activation behavior
 379 of each task $\tau_{i,j}$ contained in the global task set \mathcal{T} . Due to the existing precedence constraints

² The notation $\eta^{+l}(\Delta t)$ expresses that the maximum event model refers to the *closed* time interval $[0, t]$.



(a) Local worst case busy window with $C = \mathcal{T}_k$, $K_{i,j} = 1$

(b) Local typical worst case busy window with $C = \emptyset$



(c) Exemplary decomposition of the maximum event model $\eta_{m,n}^+(\Delta t)$ in the maximum overload event model $\eta_{m,n}^{+, (o)}(\Delta t)$ and the maximum typical event model $\eta_{m,n}^{+, (t)}(\Delta t)$ for task $\tau_{m,n}$

■ **Figure 5** Theorem 16: Generalized schedulability criterion

380 in a stream s_i , the activation behavior of any task $\tau_{i,j}$ with $j > 1$ is fully determined by
 381 the respective predecessor task and therefore in the end by the header task $\tau_{i,1}$. It is thus
 382 sufficient to include the activation behavior of the header tasks in the definition of a global
 383 combination.

384 ► **Definition 17** (Global combination). A global combination $C_g \subseteq \{\tau_{i,1} \mid \forall i : \tau_{i,1} \in \mathcal{T}\}$ is a
 385 set of header tasks which may experience both typical as well as overload activations. All
 386 other header tasks follow their typical event model.

387 Special global combinations are the *global typical combination* with $C_g = \emptyset$, and the *global*
 388 *worst case combination* with $C_g = \{\tau_{i,1} \mid \forall i : \tau_{i,1} \in \mathcal{T}\}$.

389 ► **Definition 18** (Schedulability of a global combination). We say a global combination C_g is
 390 schedulable if and only if under all possible scheduling scenarios (1) all streams can satisfy
 391 their end-to-end deadlines $D_{i,j}$ and (2) every task meets its local deadline $d_{i,j}$.

392 We require that the given event models of the header tasks are such that the following
 393 schedulability constraints are respected.

394 ► **Definition 19** (Global typical worst case). If the system behaves according to the global
 395 typical combination, then the task set \mathcal{T} is schedulable even in the most unfavorable scenario
 396 (global typical worst case).

397 ► **Definition 20** (Global worst case). If the system behaves according to the global worst
 398 case combination, the task set \mathcal{T} is possibly unschedulable in the most unfavorable scenario
 399 (global worst case).

400 We would like to mention that for computing weakly-hard real-time guarantees, naturally
 401 only systems which *are* unschedulable in the global worst case are of interest.

402 5.2 Computation of Minimum and Maximum Event Models

403 While for the header tasks the minimum and maximum event model $\eta_{i,j}^-(\Delta t)$, $\eta_{i,j}^+(\Delta t)$ is
 404 given by the system specification, it has to be derived for successor tasks $\tau_{i,j}$ with $j > 1$.
 405 The classical CPA is capable of deriving these event models for all successor tasks from
 406 the original CPA input model as defined in Section 2. Thus CPA explores here the most
 407 favorable and the most unfavorable behavior of the global worst case combination.

408 5.3 Computation of Minimum and Maximum Typical Event Models

409 The minimum and maximum typical event model $\eta_{i,j}^{-(t)}(\Delta t)$, $\eta_{i,j}^{+(t)}(\Delta t)$ have also to be
 410 computed for the successor tasks $\tau_{i,j}$ with $j > 1$. Our claim is that CPA can also be used
 411 for this purpose, given that in the input model the worst case bounds $\eta_{i,1}^-(\Delta t)$, $\eta_{i,1}^+(\Delta t)$ are
 412 replaced by the typical event models $\eta_{i,1}^{-(t)}(\Delta t)$, $\eta_{i,1}^{+(t)}(\Delta t)$. In other words, CPA is now
 413 applied for the best case and worst case scenario where all header tasks see only typical
 414 events (global typical combination). CPA, which is agnostic of event types, computes the
 415 converged minimum and maximum event models for all stream tasks. We assume in this
 416 paper that all typical events that are injected at the head of a stream keep their typical
 417 nature while propagating through the system. Knowing that only typical events have served
 418 for stream activation, we can interpret the CPA-derived event models as typical and have
 419 thus $\eta_{i,j}^{-(t)}(\Delta t)$ and $\eta_{i,j}^{+(t)}(\Delta t)$ for all stream tasks.

420 5.4 Computation of Minimum and Maximum Overload Event Models

421 Finally, our intention is to obtain the minimum and maximum overload event models for
 422 each successor task $\tau_{i,j}$ with $j > 1$. We begin by describing how an arbitrary event flow
 423 $e_{i,j}(t)$ can be decomposed in a typical event flow $e_{i,j}^{(t)}(t)$ and an overload event flow $e_{i,j}^{(o)}(t)$.
 424 In this context, we use the concept of a sliding window function which returns a maximum
 425 event model for a specific event flow.

426 ► **Definition 21** (Sliding window function). A sliding window function f_{slw} takes a specific
 427 event flow $e_{i,j}(t)$ of task $\tau_{i,j}$ defined on $0 \leq t \leq T$ as an input, and returns a maximum event
 428 model for $e_{i,j}(t)$, denoted as $\eta_{e_{i,j},T}^+(\Delta t)$ for any interval size $0 \leq \Delta t \leq T$. This maximum
 429 event model $\eta_{e_{i,j},T}^+(\Delta t)$ is derived by passing a window of size Δt over the event flow $e_{i,j}(t)$
 430 of length T and noting down the maximum number events contained in any position of the
 431 window Δt such that

$$432 \quad \eta_{e_{i,j},T}^+(\Delta t) = \max_{t_1, t_2 : 0 \leq t_1 \leq t_2 \leq T \wedge t_2 - t_1 = \Delta t} \{e_{i,j}(t_2) - e_{i,j}(t_1)\}.$$

434 ► **Theorem 22** (Decomposition of an event flow). Let $e_{i,j}(t)$ be an arbitrary event flow of
 435 length T belonging to task $\tau_{i,j}$. Known bounds for the activation frequency of task $\tau_{i,j}$ are
 436 i.a. $\eta_{e_{i,j},t}^+(\Delta t)$ for all (sub)lengths of the event flow with $0 \leq t \leq T$ and the maximum typical
 437 event model $\eta_{i,j}^{+(t)}(\Delta t)$. A valid decomposition of $e_{i,j}(t)$ in a typical and overload event flow
 438 is given by

$$439 \quad e_{i,j}^{(o)}(t) = \max_{0 \leq \Delta t \leq t} \left\{ 0, \eta_{e_{i,j},t}^+(\Delta t) - \eta_{i,j}^{+(t)}(\Delta t) \right\} \quad e_{i,j}^{(t)}(t) = e_{i,j}(t) - e_{i,j}^{(o)}(t). \quad (12)$$

441 **Proof.** The event flow $e_{i,j}(t)$ cannot contain more than $\eta_{i,j}^{+, (t)}(\Delta t)$ typical events in the
 442 observed interval $[0, t)$ by Def. 11, where $\Delta t = t - 0$. All events that occur additionally to
 443 the maximum number of typical events $\eta_{i,j}^{+, (t)}(\Delta t)$ in $[0, t)$ are a potential source of overload
 444 in the system and can therefore be safely interpreted as overload events.

445 To determine the number overload events in $e_{i,j}(t)$, we (1) apply the sliding window
 446 function to $e_{i,j}(t)$ within $[0, t)$ which results in $\eta_{e_{i,j}, t}^+(\Delta t)$, and then (2) compare point-
 447 wise $\eta_{e_{i,j}, t}^+(\Delta t)$ with $\eta_{i,j}^{+, (t)}(\Delta t)$. Pointwise comparison is done chronologically by increas-
 448 ing continuously the size of Δt with $0 \leq \Delta t \leq t$. The largest nonnegative difference
 449 $\max_{0 \leq \Delta t \leq t} \left\{ 0, \eta_{e_{i,j}, t}^+(\Delta t) - \eta_{i,j}^{+, (t)}(\Delta t) \right\}$, is the number of overload events in $e_{i,j}(t)$.

450 Why is it not sufficient to compute $\max \left\{ 0, \eta_{e_{i,j}, t}^+(\Delta t) - \eta_{i,j}^{+, (t)}(\Delta t) \right\}$ for $\Delta t = t$? Let $\Delta t'$
 451 be the first interval, where the maximum budget of typical events is exceeded by the event
 452 flow such that $\eta_{e_{i,j}, t}^+(\Delta t') - \eta_{i,j}^{+, (t)}(\Delta t') > 0$. This information should not be contradicted
 453 by a later smaller value of overload events derived at $\Delta t'' > \Delta t'$. This, however, may
 454 happen due to the cumulative representation of event arrival within Δt by event models,
 455 where information on the alignment of events gets lost with increasing interval size. The
 456 alignment information is however important to distinguish overload from typical events. The
 457 formulation $e_{i,j}^{(o)}(t) = \max_{0 \leq \Delta t^* \leq t} \left\{ 0, \eta_{e_{i,j}, t}^+(\Delta t^*) - \eta_{i,j}^{+, (t)}(\Delta t^*) \right\}$ preserves the information on
 458 the maximum number of overload events once gained at Δt^* . Also, $e_{i,j}^{(o)}(t)$ is a wide-sense
 459 increasing function which accumulates the number of occurred overload events over time, and
 460 therefore satisfies Def. 10 of an event flow. Furthermore, we have $e_{i,j}^{(t)}(t) = e_{i,j}(t) - e_{i,j}^{(o)}(t)$
 461 since an event in an event flow can either be overload or typical. ◀

462 In the following Theorem 23, we state how to compute a maximum overload event model. We
 463 would like to note that the minimum overload event model is the zero function $\eta_{i,j}^{+, (o)}(\Delta t) = 0$
 464 since overload events can be completely absent cf. global typical combination.

465 ▶ **Theorem 23** (Obtaining an overload event model). *A maximum overload event model is*

$$466 \quad \eta_{i,j}^{+, (o)}(\Delta t) = f_{slw} \left(\max_{0 \leq \Delta t^* \leq \Delta t} \left\{ \eta_{i,j}^+(\Delta t^*) - \eta_{i,j}^{+, (t)}(\Delta t^*) \right\} \right)$$

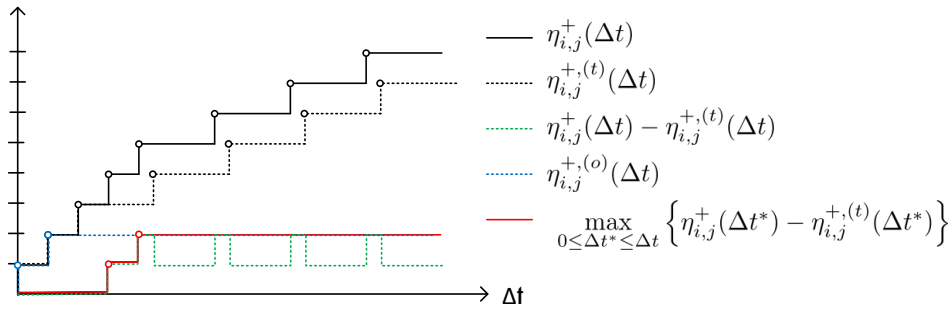
467 where f_{slw} is a sliding window function.

469 **Proof.** An upper bound for all event flow-specific maximum event models $\eta_{e_{i,j}, T}^+(\Delta t)$ of task
 470 $\tau_{i,j}$ is the maximum event model $\eta_{i,j}^+(\Delta t)$ by Def. 2. Thus we have

$$471 \quad \max_{0 \leq \Delta t^* \leq t} \left\{ 0, \eta_{e_{i,j}, t}^+(\Delta t^*) - \eta_{i,j}^{+, (t)}(\Delta t^*) \right\} \leq \max_{0 \leq \Delta t^* \leq \Delta t} \left\{ \eta_{i,j}^+(\Delta t^*) - \eta_{i,j}^{+, (t)}(\Delta t^*) \right\}.$$

473 In other words, the overload event flow $\tilde{e}_{i,j}^{(o)}(t) = \max_{0 \leq \Delta t^* \leq t} \left\{ \eta_{i,j}^+(\Delta t^*) - \eta_{i,j}^{+, (t)}(\Delta t^*) \right\}$ is always
 474 larger than any other arbitrary overload event flow $e_{i,j}^{(o)}(t)$. To derive from the largest overload
 475 event flow $\tilde{e}_{i,j}^{(o)}(t)$ the corresponding maximum overload event model, we apply once again the
 476 sliding window function such that $\tilde{e}_{i,j}^{(o)}(t_2) - \tilde{e}_{i,j}^{(o)}(t_1) \leq \eta_{i,j}^{+, (o)}(t_2 - t_1) = f_{slw} \left(\tilde{e}_{i,j}^{(o)}(t_2 - t_1) \right)$.
 477 The computation of the overload event model $\eta_{i,j}^{+, (o)}(\Delta t)$ is illustrated in Figure 6. ◀

478 Calculating a maximum overload event model according to Theorem 23 requires a high
 479 computational effort since the sliding window approach has to be applied to the infinitely
 480 long event flow $\tilde{e}_{i,j}^{(o)}(t) = \max_{0 \leq \Delta t^* \leq t} \left\{ \eta_{i,j}^+(\Delta t^*) - \eta_{i,j}^{+, (t)}(\Delta t^*) \right\}$. Fortunately most event flows



■ **Figure 6** Computing a maximum overload event model

481 have a repetitive behavior or can be approximated by repetitive functions, so that the effort
 482 to derive overload event models is significantly reduced. In the following, we discuss special
 483 and practically relevant cases for the computation of overload event models.

484 ► **Case 1 (Zero typical event model).** In this trivial but important case, the task $\tau_{i,j}$ has a
 485 zero typical event model $\eta_{i,j}^{+, (t)}(\Delta t) = 0$. Obviously, we have $\eta_{i,j}^{+, (o)}(\Delta t) = \eta_{i,j}^+(\Delta t)$. This case
 486 is relevant for header tasks, which have the character of a sporadic interferer.

487 ► **Case 2 (Zero overload event model).** In a second trivial but important case, the maximum
 488 and maximum typical event model of task $\tau_{i,j}$ are identical such that $\eta_{i,j}^+(\Delta t) = \eta_{i,j}^{+, (t)}(\Delta t)$.
 489 Consequently, we have a zero overload event model $\eta_{i,j}^{+, (o)}(\Delta t) = 0$. Header tasks with a
 490 periodic activation have often this behavior.

491 ► **Case 3 (Repetitive overload event flow).** If the overload event flow $\tilde{e}_{i,j}^{(o)}(t)$ is T -repetitive
 492 possibly with an offset (cf. Lemma 7), then applying the sliding window algorithm can be
 493 restricted to the interval $[0, 2T)$ to construct the maximum overload event model. In the
 494 following Theorem 24, we show that a T -repetitive overload event flow is obtained if the
 495 event model $\eta_{i,j}^+(\Delta t)$ and the typical event model $\eta_{i,j}^{+, (t)}(\Delta t)$ are both T -repetitive extensions
 496 (which can be achieved by appropriate output model computation described Section 3.1.2).

497 ► **Theorem 24 (Repetitive overload event flow).** *If the event model $\eta^+(\Delta t)$ and the typical*
 498 *event model $\eta^{+, (t)}(\Delta t)$ are both T -repetitive extensions, then the resulting overload event flow*
 499 *$\tilde{e}_{i,j}^{(o)}(t)$ is likewise T -repetitive, such that*

$$500 \quad \tilde{e}_{i,j}^{(o)}(t) = \max_{0 \leq \Delta t^* \leq t} \left\{ \left\lfloor \frac{\Delta t^*}{T} \right\rfloor \cdot (\eta^+(T) - \eta^{+, (t)}(T)) + \eta^+(\Delta t^* - \left\lfloor \frac{\Delta t^*}{T} \right\rfloor T) - \eta^{+, (t)}(\Delta t^* - \left\lfloor \frac{\Delta t^*}{T} \right\rfloor T) \right\}.$$

Proof.

$$502 \quad \max_{0 \leq \Delta t^* \leq \Delta t} \{ \eta^+(\Delta t^*) - \eta^{+, (t)}(\Delta t^*) \}$$

$$503 \quad = \max_{0 \leq \Delta t^* \leq \Delta t} \left\{ \left\lfloor \frac{\Delta t^*}{T} \right\rfloor \cdot \eta^+(T) + \eta^+(\Delta t^* - \left\lfloor \frac{\Delta t^*}{T} \right\rfloor T) - \left\lfloor \frac{\Delta t^*}{T} \right\rfloor \cdot \eta^{+, (t)}(T) - \eta^{+, (t)}(\Delta t^* - \left\lfloor \frac{\Delta t^*}{T} \right\rfloor T) \right\}$$

$$504 \quad = \max_{0 \leq \Delta t^* \leq \Delta t} \left\{ \left\lfloor \frac{\Delta t^*}{T} \right\rfloor \cdot (\eta^+(T) - \eta^{+, (t)}(T)) + \eta^+(\Delta t^* - \left\lfloor \frac{\Delta t^*}{T} \right\rfloor T) - \eta^{+, (t)}(\Delta t^* - \left\lfloor \frac{\Delta t^*}{T} \right\rfloor T) \right\}$$

$$505 \quad = \max_{0 \leq \Delta t^* \leq \Delta t} \left\{ \left\lfloor \frac{\Delta t^*}{T} \right\rfloor \cdot \eta^{diff}(T) + \eta^{diff}(\Delta t^* - \left\lfloor \frac{\Delta t^*}{T} \right\rfloor T) \right\}$$

507 where $\eta^{diff}(\Delta t) = \eta^+(\Delta t) - \eta^{+, (t)}(\Delta t)$.

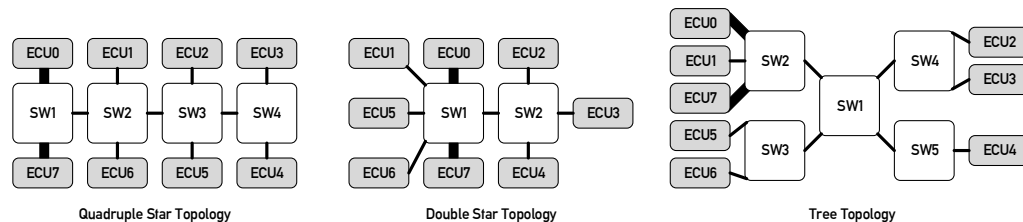
508

509 6 Experiments

510 The presented experiments focus on computing end-to-end (m, k) -guarantees for traffic
 511 streams in realistic network settings, while exploring how a varying amount of overload
 512 impacts the timing behavior of the investigated system.

513 6.1 System Generation

514 The case study presented in Thiele et al. [20] provides characteristics of future automotive
 515 backbone networks by Daimler. Based on this data, we have randomly generated a set of
 516 automotive switched Ethernet networks with mapped traffic streams. Firstly, let us present
 517 the data used from the case study. Figure 7 illustrates three possible network topologies. The
 518 topologies vary in the number of switches (SWs) which interconnect 8 electronic control units
 519 (ECUs). Links operate at 100 Mbit/s, only ECU0 and ECU7 are equipped with 1Gbit/s
 520 links due to high load. Stream characteristics are described statistically by [20], they are
 521 summarized in Table 1a. There are 50 periodic control streams of highest priority and 4
 522 periodic camera streams of lower priority. Control streams have relatively small payloads and
 523 rather long periods, while camera streams have large payloads and shorter periods. Some of
 524 the streams are unicast, others are multicast or broadcast. A periodically sent Ethernet frame
 525 is mapped to exactly one stream. Information on the frame payload as well as on periods is
 526 given by [20] only in form of minimum and maximum values, averages, and quartiles for the
 527 purpose of data anonymization. In case of camera traffic, the number of streams is too small
 528 for quantifying quartiles. IPv4/UDP is used at the network/transport layer, which adds
 529 28 bytes of protocol overhead (not shown in Table 1a). Furthermore, the communication
 530 matrix in Table 1b is given by [20] indicating the number of control and camera streams sent
 531 between a tuple of nodes. We use a parser to translate the network described in terms of
 532 topology and streams into a CPA/TWCA system model as defined in Sections 2 and 4.1.



■ **Figure 7** Network topologies. Thin lines represent links at 100 Mbit/s, while thick lines represent links at 1 Gbit/s. A maximum wire length of 10 m is assumed, which translates to a maximum wire propagation delay of 33 ns.

533 Secondly, we describe the random generation of systems which conform to the presented
 534 properties. The generation process is designed to produce a configurable number of systems
 535 and consists of several runs. A single generation run first creates the set of 54 streams with
 536 their respective source and destination ECUs, and then the streams are mapped to each of
 537 the three topologies. A run thus creates 3 systems at once. However, this set of 3 systems is
 538 discarded if at least one is not schedulable to enable meaningful comparisons between the
 539 different topologies.

540 ■ *Generation of control streams.* Periods and payloads of control streams are only described
 541 by statistic figures. Therefore, we used fitting to find distributions which come closest

	CONTROL	CAMERA
STREAMS		
# total	50	4
# unicast	26	3
# 2-cast	13	1
# 3-cast	4	0
# 4-cast	1	0
# broadcast	6	0
FRAME PAYLOAD IN BYTES		
[min, max]	[1, 250] B	[875, 1400] B
average	54 B	1231 B
quartiles	$q_{0.25} = 8$ B, $q_{0.50} = 25$ B, $q_{0.75} = 74$ B	
PERIOD		
[min, max]	[5ms, 1s]	[100us, 1ms]
average	182ms	440us
quartiles	$q_{0.25} = 10$ ms, $q_{0.50} = 40$ ms, $q_{0.75} = 175$ ms	

(a) Stream characteristics

Src/Dst	ECU0	ECU1	ECU2	ECU3	ECU4	ECU5	ECU6	ECU7
ECU0		1			1 1		10	2 2
ECU1	1							1 1
ECU2					5			
ECU3					1			
ECU4	1	2	3	3		1	1	1
ECU5							3	2
ECU6	10	6	4	3	4	3		10
ECU7	5	2	2	2	4 1	3	8	

(b) Communication matrix indicating the number of control streams (black number, 1st entry) and camera streams (blue number, 2nd entry) between a pair of ECUs.

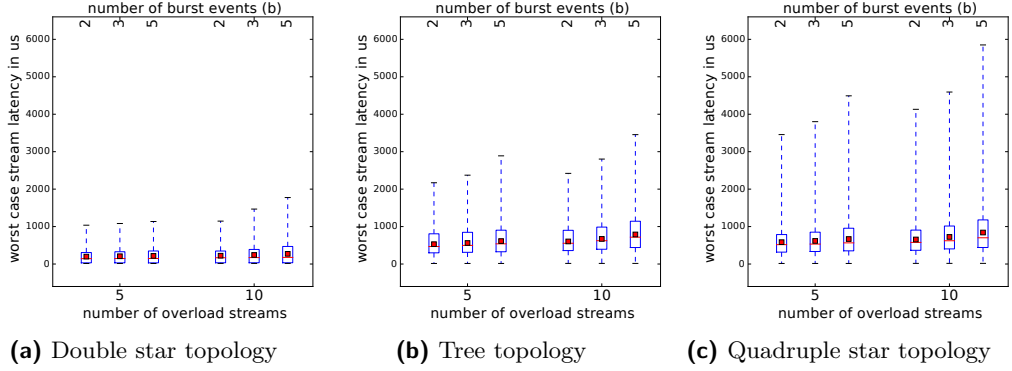
■ **Table 1** Traffic properties as given in Thiele et al. [20]

542 the indicated average and quartiles. For the periods, we opted for a Weibull distribution
 543 with the parameters $shape = 0.54$ and $scale = 88.09$. For the payload, an exponential
 544 distribution with $\lambda = 0.02$ was used.

- 545 ■ *Generation of camera streams.* The few, i.e. 4, camera streams $s_{cam,i}$ are assigned
 546 the same payloads and periods in each system generation run: $s_{cam,0} \mapsto (100\mu s, 875B)$;
 547 $s_{cam,1} \mapsto (1ms, 1400B)$; $s_{cam,2} \mapsto (330\mu s, 1325B)$; $s_{cam,3} \mapsto (330\mu s, 1325B)$.
- 548 ■ *Generation of stream sources & destinations and topology mapping.* The given communic-
 549 ation matrix defines constraints on pairs of source-destination ECUs and on the number
 550 of streams sent between them. Stream sources & destinations are generated randomly
 551 respecting these constraints. The traffic is then mapped to each of the 3 topologies,
 552 creating 3 different systems with identical streams.
- 553 ■ *Schedulability test.* For control streams, local deadlines are set to the stream period and
 554 the end-to-end deadline is the sum of the local deadlines. For camera streams, we choose
 555 arbitrarily an end-to-end deadline of $2ms$ ($s_{cam,0}$, $s_{cam,2}$, $s_{cam,3}$) or $4ms$ ($s_{cam,1}$), such
 556 that – without any overload in the system – worst case stream latencies (WCSLs) of
 557 camera streams are already close to their end-to-end deadlines.³ Local camera deadlines
 558 are derived by uniform distribution of the end-to-end deadline. Based on these timing
 559 constraints, the generated systems are filtered such that they are all schedulable as
 560 mentioned above.

561 After a generation run, we dispose of a set of 3 systems in which no overload is present. We
 562 then add sporadic control streams to each system as transient overload. We see this as a
 563 realistic extension of the system description, representing event-triggered communication.
 564 A sporadic control stream s' is a duplicate of a randomly chosen control stream s from the
 565 original stream set but with modified activation behavior. The typical activation behavior

³ The worst case stream latency (WCSL) for a unicast stream is computed by summing the WCRTs of tasks included in the stream. For multi- or broadcast streams, the WCSLs are computed separately for each path from the source to a destination.



■ **Figure 8** Worst case latencies of control and camera streams under varying topologies and overload. Each single box plot is based on the streams of 50 randomly generated systems with the indicated properties (num. of bursts, num. of overload streams).

566 of s' is zero, while the nonzero overload activation behavior is modeled as sporadically
 567 bursty [16]: A burst of b events with a minimum distance T_{in} is repeated after an outer
 568 period T_{out} such that $\eta^{+, (o)}(\Delta t) = \left\lfloor \frac{\Delta t}{T_{out}} \right\rfloor \cdot b + \min \left\{ \left\lceil \frac{\Delta t - \lfloor \frac{\Delta t}{T_{out}} \rfloor \cdot T_{out}}{T_{in}} \right\rceil, b \right\}$. While the burst
 569 length b is used as a variable parameter in the experiments, fixed parameters are $T_{in} = 100\mu s$
 570 and T_{out} is 10-times the period of the original stream s .

571 6.2 Experimental Results

572 In the experiments, we investigate the impact of overload on the timing behavior of the
 573 generated systems. For each presented overload configuration, we randomly generated 50
 574 systems of the same topology. We first present worst case stream latencies (WCSLs), and
 575 then discuss the DMMs computed for streams. The results in this section are presented
 576 in box plots as, for instance, in Figure 8a. This is done to summarize results (WCSLs or
 577 DMMs) over all streams from a set of similar systems. A single box plot indicates the average
 578 (red square) and the quartiles $q_{0.25}$, $q_{0.50}$, $q_{0.75}$ of the results. The 1st and 3rd quartiles $q_{0.25}$
 579 and $q_{0.75}$ are the top and the bottom of the blue framed box, while the red band inside the
 580 box is the 2nd quartile (median). The whiskers indicate results outside the quartiles.

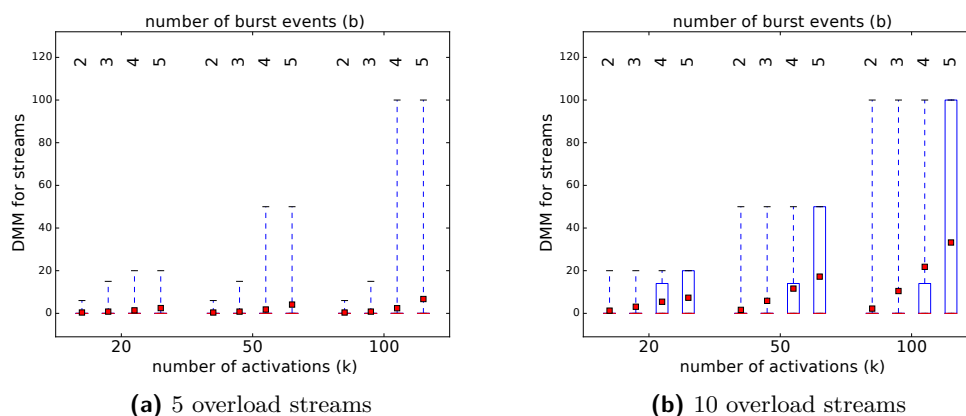
581 **Worst Case Stream Latencies.** The WCSLs depend both on the system characteristics
 582 as well as on the amount of introduced overload. Figure 8 shows that the double star topology
 583 has the shortest WCSLs, compared to to the tree topology with intermediate WCSLs and
 584 the quadruple star topology with even higher WCSLs. This behavior is due to the varying
 585 number and extent of contention points in the different topologies. Moreover, Figure 8
 586 confirms the intuition that WCSLs increase with the amount of overload in the system, which
 587 is controlled by the number of overload streams in the system and the number of burst events
 588 b of each overload stream.

589 **Deadline Miss Models of Streams.** While the control streams satisfy their end-to-end
 590 deadlines even in the presence of overload, camera streams suffer from occasional deadline
 591 misses in particular in case of the quadruple star topology. A deadline miss in the context of
 592 a camera stream can be interpreted as a frame loss which impacts then video quality. We
 593 therefore focus on the DMMs of the camera streams. Figure 9 illustrates the DMMs for all
 594 camera streams of generated systems with quadruple star topology. Overload is varied by
 595 the number of overload streams and the burst length. We compute the DMM of a unicast

596 stream as the sum of the task DMMs included in the stream. In the case that one or more
 597 local deadlines are violated but the global deadline is satisfied, the stream DMM is set to
 598 zero. Multicast and broadcast streams are decomposed into unicast streams in order to
 599 compute the DMMs according to the above rule. Figure 9a indicates DMMs for camera
 600 streams in the presence of 5 sporadic overload streams, while Figure 9b shows DMMs for
 601 an increased number of 10 sporadic overload streams. Table 2 lists the nonzero DMMs
 602 results for $k = 100$ to get a more detailed impression of the individual weakly-hard real-time
 603 guarantees. The number of deadline misses grows as expected with the number of overload
 604 streams. Furthermore, the m - k -ratio is improving for growing k .

- 605 ■ For 5 overload streams many camera streams are schedulable for any burst length. Few
 606 systems have camera streams that are not schedulable. Among these systems with late
 607 camera streams, most of them have a very acceptable (m, k) behavior – in particular for
 608 $b \in \{2, 3\}$.
- 609 ■ For 10 overload streams more camera streams experience occasional deadline misses. For
 610 $b \in \{2, 3\}$, the maximum number of deadline misses m in k executions is acceptable
 611 for many camera streams depending on system requirements. For $b \geq 4$ many of the
 612 investigated systems are clearly overloaded.

613 A note on run times: On a PC with an Intel i5-4210M processor at 2.6 GHz and 8GB RAM,
 the analysis of a single system is in the order of 15-30 seconds.



614 ■ **Figure 9** DMMs for camera streams under varying overload for the quadruple star topology.
 Results evaluate camera streams in 50 systems. For a multicast camera stream with n destinations,
 there are n end-to-end DMMs computed.

614

615 **7** Related Work

616 The seminal paper by Bernat et al. [1] has presented the principles of weakly-hard real-time
 617 systems. It summarizes existing work in a similar direction, introduces (m, k) -constraints,
 618 and derives (m, k) -guarantees for periodic task sets with known offsets under fixed priority
 619 scheduling. More powerful verification techniques for weakly-hard real-time systems have
 620 been subsequently developed. In particular, Quinton et al. [14] has introduced a method
 621 called TWCA, which can handle more comprehensive system models covering, e.g., arbitrary
 622 activation event models. The initial work [14] has been extended and refined in a sequence of
 623 publications; the latest analysis version is presented in [21]. A new and recent development

bursts	nonzero dmm(100) results with number of occurrence n in brackets (n)
5 overload streams	
$b = 2$	2(6), 3(5), 4(15), 6(2)
$b = 3$	2(6), 3(5), 4(22), 5(1), 6(1), 7(6), 9(1), 13(1), 15(1)
$b = 4$	2(2), 3(3), 4(19), 5(4), 6(1), 7(1), 8(2), 9(1), 10(3), 11(2), 12(1), 13(1), 14(1), 16(1), 18(1), 30(1), 100(3)
10 overload streams	
$b = 2$	2(2), 3(2), 4(31), 5(1), 6(6), 11(2), 12(1), 14(1), 16(1), 19(1), 100(3)
$b = 3$	4(15), 5(5), 7(2), 8(1), 9(1), 10(2), 12(5), 14(2), 15(4), 16(2), 100(23)
$b = 4$	4(2), 5(1), 8(1), 9(3), 10(1), 13(2), 14(10), 16(1), 20(2), 21(2), 30(1), 100(51)

■ **Table 2** Details on nonzero DMM results for camera streams for $k = 100$

624 is the verification technique for weakly-hard real-time systems presented by Sun et al. [19].
625 The work by Sun et al. [19] has only a limited focus on systems with fully periodic tasks with
626 unknown offsets under fixed priority scheduling, but it has a higher accuracy than TWCA
627 since it provides exact results. However, all of the verification techniques are restricted to
628 systems with a single service-providing resource. In this paper, we lift this restriction by
629 integrating TWCA as local analysis technique in the context of the CPA framework [11].
630 CPA is an established compositional analysis framework, which uses for each component
631 a dedicated scheduling analysis and specifies the coupling of the component-based results.
632 The advantage of using a compositional analysis framework is that large and heterogeneous
633 systems can be analyzed. The choice of the combination (TWCA, CPA) is due to the
634 similarities in the system models and interface definitions, which reduces the number of
635 compatibility issues.

636 8 Conclusion

637 In this paper, we presented TypicalCPA which is the first verification method for weakly-hard
638 real-time systems with *multiple* resources and we evaluated it in a network context with traffic
639 streams. Previous verification techniques providing weakly-hard real-time guarantees have
640 aimed at systems with only a single service-providing resource. The method builds on (1)
641 CPA, a compositional performance verification framework for hard real-time guarantees, and
642 (2) TWCA, an analysis method which derives weakly-hard real-time guarantees for systems
643 with a single resource. CPA allows to use different local scheduling analysis techniques for
644 each component in the investigated system, and defines a coupling mechanism between the
645 results provided by each component analysis. We have interpreted TWCA as such a local
646 scheduling analysis technique, but we had to extend (1) elements of TWCA as well as (2)
647 the existing coupling mechanism to achieve compatibility of both CPA and TWCA. In
648 particular, the computation and propagation of typical and overload event models between
649 tasks on different resources has been introduced. In an industrial case study, focusing on
650 automotive switched Ethernet networks, we demonstrated the applicability of TypicalCPA
651 to realistic problems. In the future, we intend to work on improved accuracy of the provided
652 weakly-hard real-time guarantees.

References

- 653 1 Guillem Bernat, Alan Burns, and Albert Liamsi. Weakly hard real-time systems. *IEEE*
654 *transactions on Computers*, 50(4):308–321, 2001.
- 655 2 Rainer Blind and Frank Allgöwer. Towards networked control systems with guaranteed
656 stability: Using weakly hard real-time constraints to model the loss process. In *Decision*
657 *and Control (CDC), 2015 IEEE 54th Annual Conference on*, pages 7510–7515. IEEE, 2015.
- 658 3 Robert I Davis, Alan Burns, Reinder J Bril, and Johan J Lukkien. Controller area network
659 (can) schedulability analysis: Refuted, revisited and revised. *Real-Time Systems*, 35(3):239–
660 272, 2007.
- 661 4 Jonas Diemer, Philip Axer, and Rolf Ernst. Compositional performance analysis in python
662 with pycpa. *Proc. of WATERS*, 2012.
- 663 5 Jonas Diemer, Philip Axer, Daniel Thiele, and Johannes Schlatow. pyCPA. URL: <https://pycpa.readthedocs.io/en/latest/index.html#>.
- 664 6 Jonas Diemer, Jonas Rox, and Rolf Ernst. Modeling of ethernet avb networks for worst-case
665 timing analysis. *IFAC Proceedings Volumes*, 45(2):848–853, 2012.
- 666 7 Jonas Diemer, Daniel Thiele, and Rolf Ernst. Formal worst-case timing analysis of ethernet
667 topologies with strict-priority and avb switching. In *Industrial Embedded Systems (SIES),*
668 *2012 7th IEEE International Symposium on*, pages 1–10. IEEE, 2012.
- 669 8 Goran Frehse, Arne Hamann, Sophie Quinton, and Matthias Woehrle. Formal analysis of
670 timing effects on closed-loop properties of control software. In *Real-Time Systems Sym-*
671 *posium (RTSS), 2014 IEEE*, pages 53–62. IEEE, 2014.
- 672 9 Mongi Ben Gaid, Daniel Simon, and Olivier Sename. A design methodology for weakly-hard
673 real-time control. *IFAC Proceedings Volumes*, 41(2):10258–10264, 2008.
- 674 10 Zain AH Hammadeh, Sophie Quinton, and Rolf Ernst. Extending typical worst-case ana-
675 lysis using response-time dependencies to bound deadline misses. In *Proceedings of the 14th*
676 *International Conference on Embedded Software*, page 10. ACM, 2014.
- 677 11 Rafik Henia, Arne Hamann, Marek Jersak, Razvan Racu, Kai Richter, and Rolf Ernst.
678 System level performance analysis—the symta/s approach. *IEE Proceedings-Computers and*
679 *Digital Techniques*, 152(2):148–166, 2005.
- 680 12 Jean-Yves Le Boudec and Patrick Thiran. *Network calculus: a theory of deterministic*
681 *queuing systems for the internet*, volume 2050. Springer Science & Business Media, 2001.
- 682 13 John P Lehoczky. Fixed priority scheduling of periodic task sets with arbitrary deadlines.
683 In *Real-Time Systems Symposium, 1990. Proceedings., 11th*, pages 201–209. IEEE, 1990.
- 684 14 Sophie Quinton, Matthias Hanke, and Rolf Ernst. Formal analysis of sporadic overload in
685 real-time systems. In *Proceedings of the Conference on Design, Automation and Test in*
686 *Europe*, pages 515–520. EDA Consortium, 2012.
- 687 15 Parameswaran Ramanathan. Overload management in real-time control applications using
688 (m, k)-firm guarantee. *IEEE Transactions on Parallel and Distributed Systems*, 10(6):549–
689 559, 1999.
- 690 16 Kai Richter. *Compositional Scheduling Analysis Using Standard Event Models*. PhD thesis,
691 TU Braunschweig, IDA, 2005.
- 692 17 Simon Schliecker, Jonas Rox, Matthias Ivers, and Rolf Ernst. Providing accurate event
693 models for the analysis of heterogeneous multiprocessor systems. In *Proceedings of the*
694 *6th IEEE/ACM/IFIP international conference on Hardware/Software codesign and system*
695 *synthesis*, pages 185–190. ACM, 2008.
- 696 18 Simon Schliecker, Jonas Rox, Matthias Ivers, and Rolf Ernst. Providing accurate event
697 models for the analysis of heterogeneous multiprocessor systems. In *Intern. Conference*
698 *on HW/SW Codesign and System Synthesis. Proceedings*, pages 185–190, New York, 2008.
699 ACM.
- 700
701

- 702 **19** Youcheng Sun and Marco Di Natale. Weakly hard schedulability analysis for fixed priority
703 scheduling of periodic real-time tasks. *ACM Transactions on Embedded Computing Systems*
704 (*TECS*), 16(5s):171, 2017.
- 705 **20** Daniel Thiele, Philip Axer, Rolf Ernst, and Jan R Seyler. Improving formal timing analysis
706 of switched ethernet by exploiting traffic stream correlations. In *Proceedings of the 2014*
707 *International Conference on Hardware/Software Codesign and System Synthesis*, page 15.
708 ACM, 2014.
- 709 **21** Wenbo Xu, Zain AH Hammadeh, Alexander Kröller, Rolf Ernst, and Sophie Quinton.
710 Improved deadline miss models for real-time systems using typical worst-case analysis. In
711 *Real-Time Systems (ECRTS), 2015 27th Euromicro Conference on*, pages 247–256. IEEE,
712 2015.